Mass Transfer Studies at the Inner Wall of an Annular Conduit in the Presence of Fluidizing Solids with Coaxially Placed Spiral Coil as Turbulence Promoter

Ratna Srinath Rao B[1]
Department of Chemical Engineering
Andhra University College of Engg.(A)
Visakhapatnam, AP, India

T Penta Rao[2]
Department of Chemical Engineering
Andhra University College of Engg.(A)
Visakhapatnam, AP, India

P Rajendra Prasad
Professor
Department of Chemical Engineering
Andhra University College of Engg.(A)
Visakhapatnam, AP, India

V. Sujatha
Professor & HOD,
Department of Chemical Engineering
Andhra University College of Engg.(A)
Visakhapatnam, AP, India

***Abstract*: Ionic mass transfer studies on the inner wall of an annular conduit in batch fluidized with the effect of coaxially placed entry region spiral coil, as turbulence promoter has been presented in this paper. Mass transfer data were obtained in annular conduit using an electrochemical technique with a potassium ferri-ferro cyanide redox system and excess sodium hydroxide was chosen as system of the study. Mass transfer coefficients were evaluated from measuring limiting currents. The study covered wide range of parameters like effect of pitch, effect of length, diameter of the coil and diameter of the coil wire, diameter of the annular rod, and particle diameter on mass transfer were studied.**

Keywords: Mass transfer, annular conduit, entry region spiral coil, turbulence promoter, augmentation

INTRODUCTION

Reduction in equipment size has an advantage of lower fixed costs for a particular duty. Consequently lowering the unit product cost. To achieve these objective several investigators has been working. Quite a few methods were employed and found significant improvements in the heat and mass transfer rates and simultaneous increase in energy losses has been reported. A balance has to be made between augmentation of mass and momentum transfer. In pursuit of this, use of annular rod, annular rod with surface modification, axially displaced promoters like spiral coils[1], twisted tapes [2], cross flow objects like cylinders [3], spheres [4], and cones [5] were employed. Rotations, vibration of transfer surfaces were also employed and enhancements were reported. Applications of additives were also employed in augmenting their processes.

Several workers employed entry region swirl generators for lowering the frictional losses while enhancing
mass transfer. Nageswara Rao, V [6] employed entry region twisted tape to generate swirl motion for the augmentation of mass transfer. Murali Mohan. V [7] employed entry region coil, coil-disc promoters achieved 4 fold augmentations over Lin et al for smooth tube with no turbulence promoter. Rao, T. P [8] employed entry region spiral coil in annular conduits and obtained an augmentation of 12 fold over Lin et al [9]. Use of fluidization for augmenting mass transfer has been employed by several workers [10-12].

Mass transfer on the inner wall of an annular conduit with batch fluidization beds with entry region swirl generators have not been reported earlier. Hence an attempt is made to obtain the effect of fluidizing solids in annular conduits with entry region coil as swirl generators.

The objective of this work is to obtain the effect of geometric parameters on mass transfer coefficients at the inner wall of annular conduits with entry region spiral coil as turbulence promoter. The geometric parameters studied are length of the coil (Lc), diameter of the coil (Dc), pitch of the coil (P_C), diameter of the coil wire (Dw), particle diameter (dp) and void fraction.

EXPERIMENTAL SET UP

Schematic diagram of experimental set up were shown in figure 1.3. The layout is similar to that used in earlier studies [1, 2, 3, 4 and 5]. It essentially consisted of a recirculation tank, an entrance calming section (A), a test section(B), an exit calming section (C), thermo wells

(E_1, E_2), flanges (F_1,F_2), gland nuts (G_1 to G_4), coiled copper tube (H), pump (P), rotameter (R), recirculation tank (T), U tube manometer (UM) and valves (V_1 to V_5).

The recirculation tank was a cylindrical copper vessel of 100 liter capacity with a drain pipe and a gate valve (V_1) for periodical cleaning of the tank. A copper coiled tube (H) with perforations was provided to bubble nitrogen through the electrolyte. The tank was connected to the pump with a 0.025 m diameter copper pipe on the suction line of the centrifugal pump. The suction line was also provided with a gate valve (V_2). The discharge line from the pump divided into two. One served as a bypass line and controlled by valve (V_3). The other line connected the pump to the entrance calming section (A) through rotameter. The rotameter was connected to a valve (V_4) for adjusting the flow at the desired rate. The rotameter has a range of 0 to $3.47x10^{-6}$ m^3/s. The entrance calming section was circular copper pipe of 0.046 m ID and 1.35m long provided with a flange and closed at the bottom with a gland nut (G_1). The entrance calming section was filled with capillary tubes to damp the flow fluctuations and to facilitate steady flow of the electrolyte through the test section.

The details of the test section were shown in figure 1.5. It was made of graduated perspex tube of 0.68 m length The diameter of the exit calming section was also of the same diameter of the entrance calming section made of copper tube of 0.05 m long, and it was provided with a flange on the upstream side for assembling the test section. It has gland nuts (G_2, G_3) at the top and bottom ends. The 0.046 m ID column through which the electrolyte was pumped was constructed by assembling the three sections the entrance calming section, the test section and the exit calming section with the flanges F_1, F_2 and the gland nuts G_1 to G_4. Two thermo wells (E_1, E_2) were provided, one at upstream side of the entrance calming section and the other at the downstream side of exit calming section to measure the temperature of the electrolyte. The coil is fixed at the entrance of the test section with the help of flanges. The central rod was placed inside the column from top to bottom in the present study and data was taken on it. Central rod was a PVC pipe of different diameter viz. 0.0127, 0.0195, 0.0254 m with equal length, 2 m. The point electrodes were made out of a copper rod of diameter $3.50x10^{-3}$ m, total of 26 point electrodes of 0.01m length were made and each electrode was soldered at one end with an insulated copper wire of sufficient length. 26 holes with a diameter slightly less than point electrodes were made on one side of the pipe starting 1.35 m from bottom of the pipe at equal spacing of 0.0254m. Carefully each soldered point electrode was flushed in to the hole and wire was taken out from one end of the pipe. (Figure 1.4)

The entry region coil was a spiral coil made from a copper wire ranging from 0.006 to 0.008m, thickness. The copper wire was coiled to a spiral coil of 0.09m to 0.16 m diameter of varying lengths and pitches of the coils were varied as 1.6, 2.6, 3.6, 4.6 cm. The spiral coil was welded to a flange and placed concentrically in the test section and fixed via flanged joints. A wire mesh was inserted by means of flanged joint which serve to hold the fluidized solids. (Figure: 1.2)

Details of the entry region coil, promoters used were compiled in the Table 1.1, respectively. Motwane make multimeter of 0.01 mA accuracy was used as an ammeter and a multimeter was acted as voltmeter. They were used for measuring the limiting current and potential measurements respectively. The other equipment used in circuit was rheostat, key, commutator, selector switch. And a lead acid battery used as the power source. The commutator facilitated the measurement of limiting currents for reduction process under identical operating conditions, while the selector switch facilitated the measurements of limiting currents at any desired electrode. The circuit diagram used for the measurement of limiting currents was shown in the figure: 1.1.

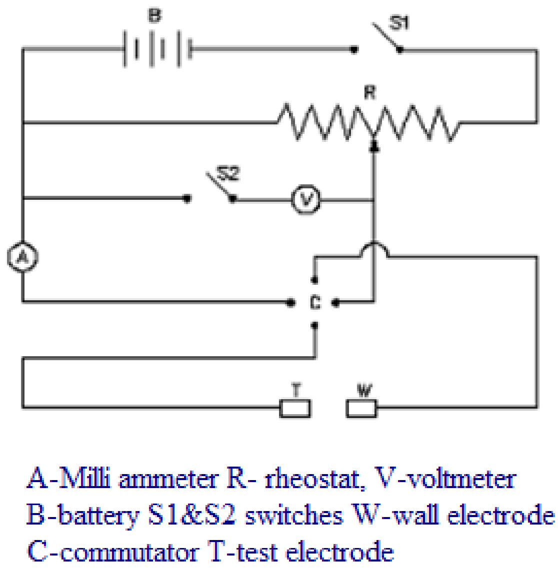

Figure 1. 1 Circuit Diagram

ENTRY REGION COILS

FIGURE1.2: PHOTOGRAPH OF TURBULENCE PROMOTERS

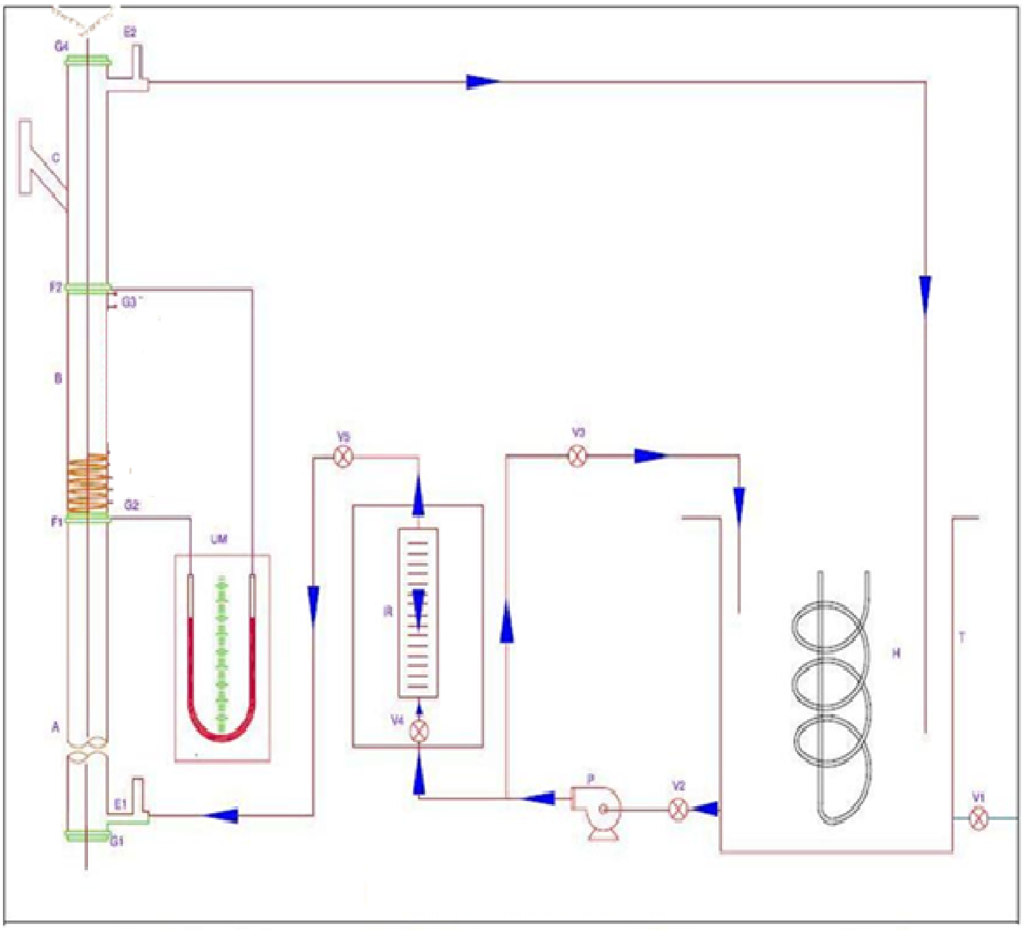

A : Entrance calming section	H : Coiled copper tube
B : Test section	P : Pump
C : Exit calming section	R : Rota meter
E_1, E_2 : Thermo wells	T : Recirculation tank
G_1 to G_4 : Gland nuts	UM : U tube manometer
F_1, F2 : Flanges	V_1 to V_5 : Valves

Figure 1.3: SCHEMATIC DIAGRAM OF EXPERIMENTAL SET UP

Figure 1. 4: CENTRAL RODS PLACE IN CIRCULAR CONDUITS

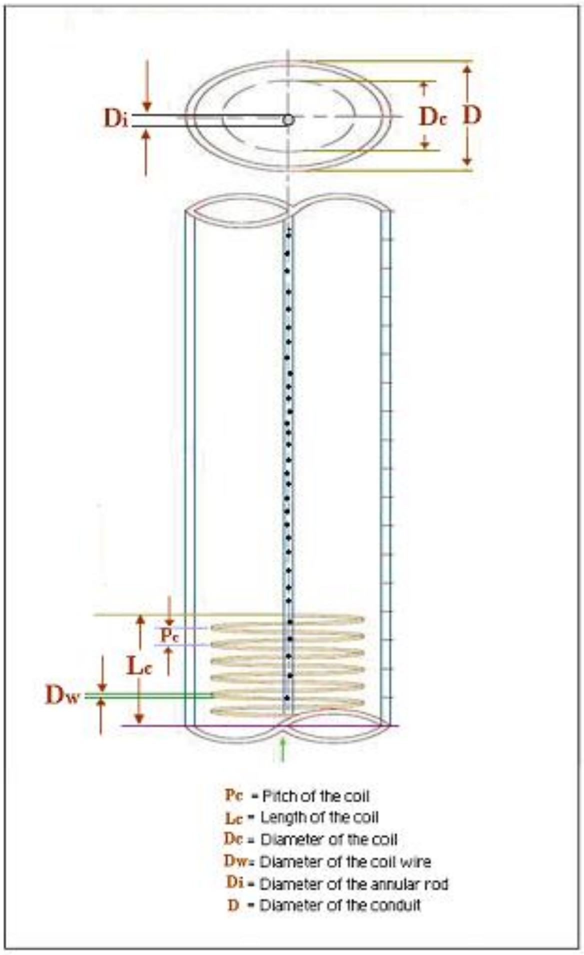

Figure1. 1.5: Details of the test section

Table: 1.1 Range of variables covered in the present study

Variable	Minimum	Maximum
Pitch of the coil (P_c), m/turn	0.016	0.046
Length of the coil (L_c), m	0.09	0.16
Diameter of the coil (D_c), m	0.031	0.038
Diameter of the coil wire (D_w), m	0.006	0.008
Diameter of the annular rod (D_i), m	0.0127	0.0254
Particle Diameter (dp),m	0.004	0.006

Experimental Procedure

80 L of the electrolyte is prepared in the storage tank using analytical grade chemicals. The electrolyte consisted of 0.01 N potassium ferricynide and 0.01 N potassium ferrocyanide with an excess 0.5 N sodium hydroxide. The electrolyte is pumped into the coloum through the rotameter with the help of the centrifugal pump. After the flow of the electrolyte is stabilized, the limiting current data are measured for reduction of ferricyanide ion at microelectrodes as described earlier [9]. Negligible change in current for considerable increase in potential indicates the attainment of limiting current. This current value corresponds to the limiting current. The electrochemical reaction occurring at the surface of the electrode is:

$$[Fe\,(CN)_6]^{-3} + e^- \text{-------------} [Fe\,(CN)_6]^{-4}$$

Three different size glass spherical particles were used as the bed material. The sphere diameter was measured with micrometer screw gauge, which has an accuracy of 0.001 inch. The average value of about 100 measurements was taken for evaluating the particle diameter.

Known volume of particles was added to the bed and the bed was expanded to a predetermined level and the corresponding flow rate was recorded. After the steady state was attained, potential was applied across the test electrode and wall electrode in small increments of potential (100mV) and the corresponding current values were measured for each increment. As the area of the wall electrode was relatively large in relation to the area of the test electrode, nearly constant potential was obtained at the test electrode. Since the potential values are not of criteria in the present study, the limiting currents were only determined from the current and potential data of applied potentials and currents as has been done in several earlier works [3, 4, 5, 6 and 7]. Flow rate, pressure drop and limiting currents were again measured. This procedure of progressive of solids was repeated to obtain data at decreasing void fraction

Mass transfer coefficients were computed from the measured limiting currents by the following equation:

$$k_L = \frac{i_L}{n\,F\,AC_o}$$

Pressure drop measurements for each flow rate were made simultaneously by using a U – tube manometer with Carbon tetrachloride as manometer liquid.

The void fraction of the fluidized beds (ε) was determined from the solids fraction calculated from the measured solids volume in the bed and effective volume of the fluidized bed. The effective volume of the fluidized bed is the total observed volume of fluidized bed less the volume of the promoter submerged in fluidized bed. Thus

Solids fraction (1- **ϵ) =V_s/V_c,**

$\epsilon = 1 - V_s/V_c$

Where V_s= volume of the solids and V_c= volume of the conduit

The void fraction of the bed for each addition of solids was evaluated from equation. The graduated transparent Perspex test section facilitated the measurement of the bed height and observation of particle distribution in fluidized bed.

RESULT AND DISCUSSIONS

Effect of promoter on mass transfer

Local variation of mass transfer along the length of the column:

Local mass transfer coefficient values are computed from measured local limiting currents and plotted against distance from the start of the coil which commences from the starting point of the test section. Mass transfer values are fluctuating little with distance indicating oscillatory behavior, but the oscillation tendency is dampened with the length of the test section. It reveals the following information.

Augmentations are largely uniform along the length of the test section. The augmentation is continuous and nearly uniform with small fluctuations when observed along the length of the column. For much longer distances, the mass transfer coefficient values would have been decreased if the study continues further along the length of the column and it is supposed to reach that of the conduits with no promoter and no solids. The local K_L values were arithmetically averaged and are nearly coinciding with the values computed with integral averaging method and used in the further analysis. Mass transfer coefficients are nearly increased with increase in the velocity. At higher velocities, declining tendency was shown. The data was analyzed in terms of dynamic and geometric parameters of the study.

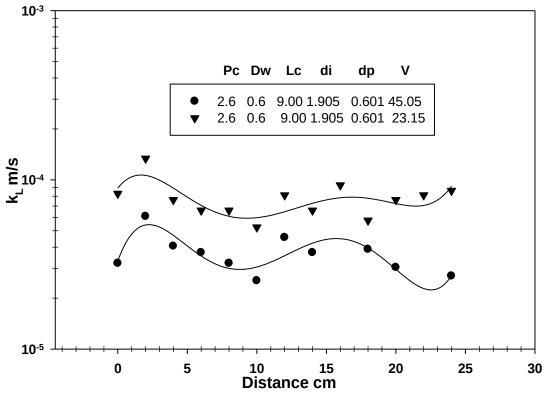

Fig1:Local Variation of Mass Transfer Coefficient along the Length of the Column

Augmentation capacity of the promoter:

The efficiency of the promoter could be adjudged by the observation of Figure-2. The figure reveals 8 to 9 fold augmentation over Lin et al, lower at a velocity of 0.2 m/s while that is tapered off -8 to 14 fold at a velocity of 0.5 m/s. It can also be observed that the fluidizing solids have larger augmentation at lower velocities while that merges with the data of k_L in annular conduits with promoter at lower solids fraction. The conduit with the coil parameters mentioned the braces were found the best augmenting promoter combination covered in the present study (P_c=4.6, D_c=3.8, D_w=0.6cm,L_c=16cm, dp=0.06cm).

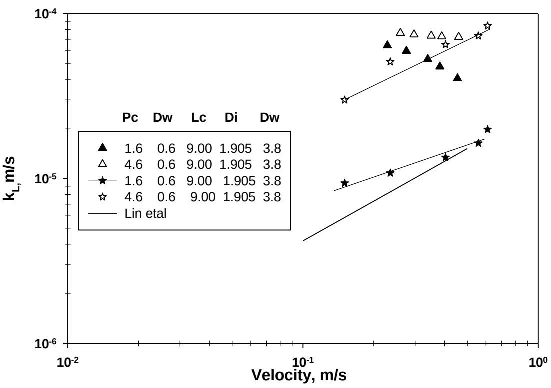

Fig 2 : Augmentation capacity of the promoter

Effect of particle diameter:

A careful observation of figure 3 reveals the effect of particle diameter. The mass transfer rates are increase with the increase in particle diameter. The augmentation values range from 1.6 to 2.4 fold at velocity of 0.2 m/s while that ranges from 3.5 to 5.6 fold at a velocity of 0.5 m/s. over batch fluidized bed with no promoter. Unlike batch fluidized beds the k_L values are marginally decreasing with velocity indicating higher augmentations at lower velocities. It can be attributed to the decrease in terminal velocities due the presence of the coil. The effect of swirl is intense and highly useful at lower velocities. Lean and stable fluidized bed could be maintained at higher velocities while harnessing higher augmentations.

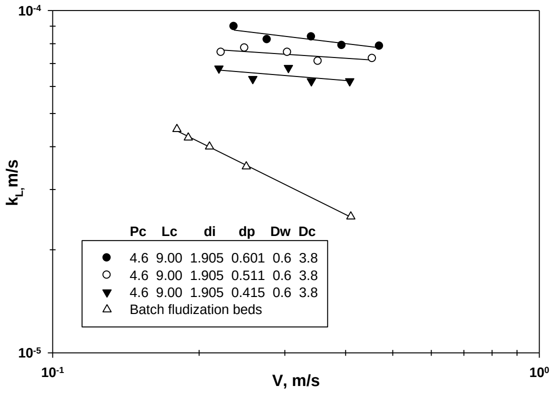

Fig 3: Effect of Particle Diameter

Effect of pitch of coil:

Effect of pitch can be seen in fig 4. At any velocity, the figure reveals that the mass transfer coefficient is increasing with pitch of the coil. At lower velocity i.e. at higher solids fraction, Pitch has strong influence; the augmentation is higher over Lin et al. for the pitches of 3.6 and 4.6. It is due to the swirl flow. The swirl effect is stronger at higher pitches. Lower augmentations are observed for lower pitches. As the velocity increases the mass transfer coefficient are decreased. It may be attributed to improper distribution of solids (or) solids may occupy dead zone. At higher pitches swirl is sufficiently intense making the particles to flow in swirl motion and the bed is more uniform. Within the range of variables covered in the study the pitch 4.6 is performing better.

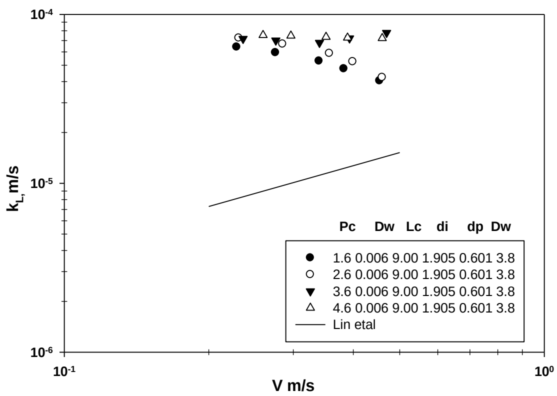

Fig 4: Effect of the pitch of the coil

Effect of Length of the Coil (L_C):

Effect of length of the coil could be demonstrated in the figure 5A & 5B. The figure reveals as the coil length increases the mass transfer coefficient decreases to a minimum followed by a raise. Indicating coil length 16cm is better augmenting for the present study. At higher pitches and at higher velocities the augmentations are better while that for lower pitches and higher velocities the enhancements are decreasing. The decrease is prominent at higher velocities.

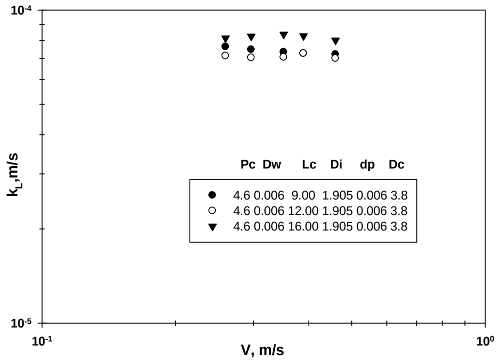

Fig 5A: effect of length of coil

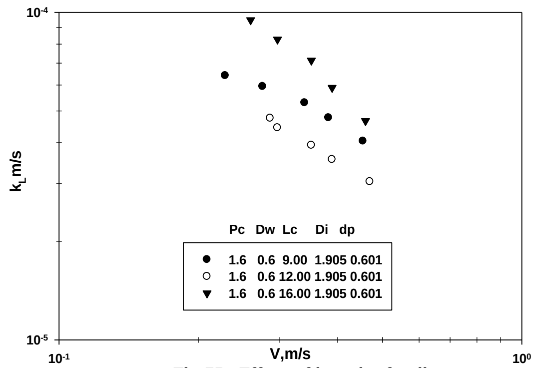

Fig 5B :Effect of length of coil

Effect of diameter of the coil:

Effect of diameter of the coil can be seen from figure 6. A marginal increase is mass transfer coefficient (k_L) is observed, indicating k_L is less sensitive with coil diameter (Dc). It may be due to it's presence in turbulent core region of the velocity profile and its variation is marginal in the present study because of lower gaps exists in annular space. At lower velocities the augmentations are marginally higher due to the prominence of swirl flow.

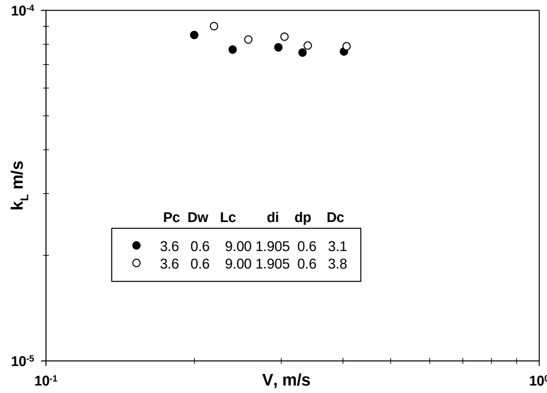

Fig 6 Effect of Coil Diameter

Figure 7 is graph for mass transfer coefficient versus porosity. k_L is decreasing with increasing in porosity. The decrease is gradual and extending up to 0.9 without entrainment. It can be concluded that lean bed could be operated with high porosity. It may reduce energy losses without much loss to enhancements.

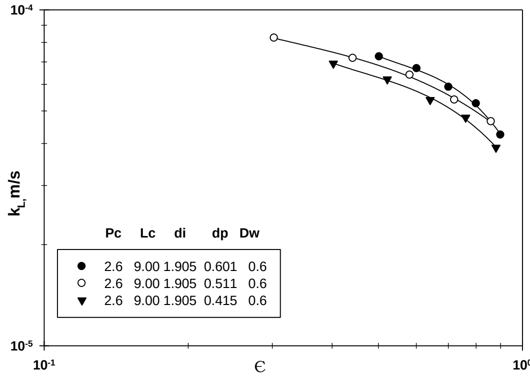

Fig 7

Figure 8 is a graph of velocity versus porosity. Porosity is increasing with velocity. The slope of the graph is found to be 1.8 to 2.0. At higher porosity the plots are merging together.

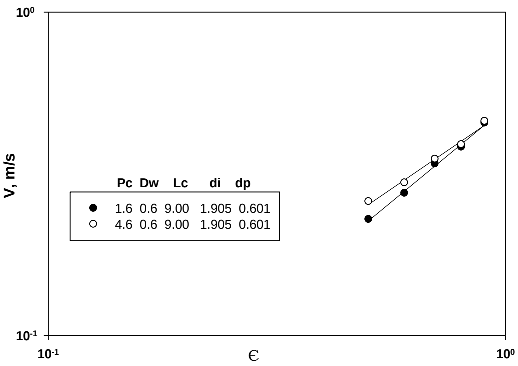

Fig 8

Observation of Figure 9 reveals the effect of velocity on voidage function. The figure exhibits a linear relationship between velocity Versus vodiage function. The voidage function is varying slightly in the lean phase, the bed is stable and could be operated without losing any solids.

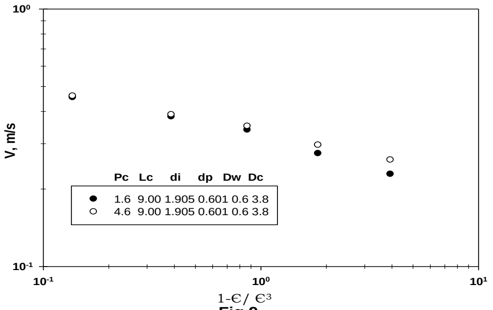

Fig 9

CONCLUSIONS:

1. Mass transfer coefficient is nearly equal with increasing in velocity. At lower pitches, mass transfer is decreasing with increase in velocity which is not desirable.
2. Mass transfer coefficient is increased with increase in pitch. The pitches 3.6 and 4.6 are better augmenting one. The pitches 1.6, 2.6 have shown a decreasing tendency.
3. Mass transfer coefficients are decreased to a minimum at 12 cm length of the coil followed by an increase. The length 16 cm is augmenting better.
4. The effect of mass transfer coefficient on the diameter of the coil is marginal because of marginal variation is only possible.
5. The present study shows maximum augmentation of 14 fold over Lin et al and 1.58 folds over entry region coil without solids.
6. Mass transfer coefficient increase with increase in diameter of the particle (d_p).
7. Porosity could be maintained up to 0.9 without any loss of particles.

NOMENCLATURE

A = Area of electrode, m^2
c = concentration of electrolyte, kg-mole/ m^3
c_l = length of the conduit, m
d = diameter of the conduit, m
d_e = Equivalent diameter,m
D = diffusion coefficient, m^2/ s
D_e = eddy diffusivity, m^2/ s
F = faraday's constant = 96,540 coulombs/ g-mole
I_L = limiting current density, amps
k_L = mass transfer coefficient, m/s
L_c = Length of the coil, m
N = mass flux
P_c = Pitch of the coil, m/turn
R = radius of the conduit, m

REFERENCES

1. Vaka Murali Mohan., S.sarveswara Rao and Rajendra Prasad.P. AIChE Annual Meeting, salt lake city , Utah, Nov 4-9, 2007, pp 2123-2130
2. Ventsislav Zimparov
Int. J of Heat and Mass Transfer, Vol 47/3, Jan 2004, pp 589-599.
3. Lin, C, S., Denton, E, B., Gaskill, H, S and Putnam, G, L Industrial and Engineering Chemistry, vol. 43, no 9, Sep 1951, pp2136-2143.
4. Chiou, J, P.
Trans.A.S.M.E., vol 109, may 1987, pp 300-307.
5. Rajendra Prasad, P.
"Ph.D Thesis, Andhra University, Visakhapatnam, INDIA. 1993.
6. Rajendra Prasad, P., Sujatha,V., Sarma, C, B and Raju, G, J, V, J
Chemical Engineering and Processing J, vol 43, 2004, pp 1055 -1062.
7. Sujatha, V., Bhaskara Sarma, C and Jagannadha Raju, G, J, VChemical Engineering and Processing J, Vol 36/1, Feb 1997, pp 67-73.
8. Webb, R, L., Eckert, R, G and Goldstein, R, J Int. J of Heat and Mass Transfer, Vol 14/4, April 1971, pp 601-617.
9. Dipprey, D, F and Sabersky, R, H Int. J of Heat and Mass Transfer, Vol 6/5, May 1963, pp 329-332.
10. 10.Nikuradse,J "Laws of flow in rough pipes"
VDI Forsch, 361, 1933.
11. R.G. Deissler,
Nat. Adv. Comm. Aeronaut., Washington, DC, TN-1210, 1955.
12. R.G. Deissler, C.S. Eian,
Nat. Adv. Comm. Aeronaut., Washington, DC, TN-2629, 1952.
13. S.L. Lyons, T.J. Hanratty, J.B. McLaughlin
Int. J. Heat and Mass Transfer, 34, 1991, pp 1149-1158.
14. Aravinth, S
Int. J. of Heat and Mass Transfer, Vol 43/8, Apr 2000, pp 1399-1408.
15. G.A. Hughmark,
Ind. Eng. Chem. Fundamentals 8, 1969, pp 31-35.
16. Vonkarman, T, H
Transactions of the A S M E, 1939, pp 705-710.
17. E.M. Sparrow, J.A. Malina,
Chemical Engineering Science Journal 19, 1964, 953-962.